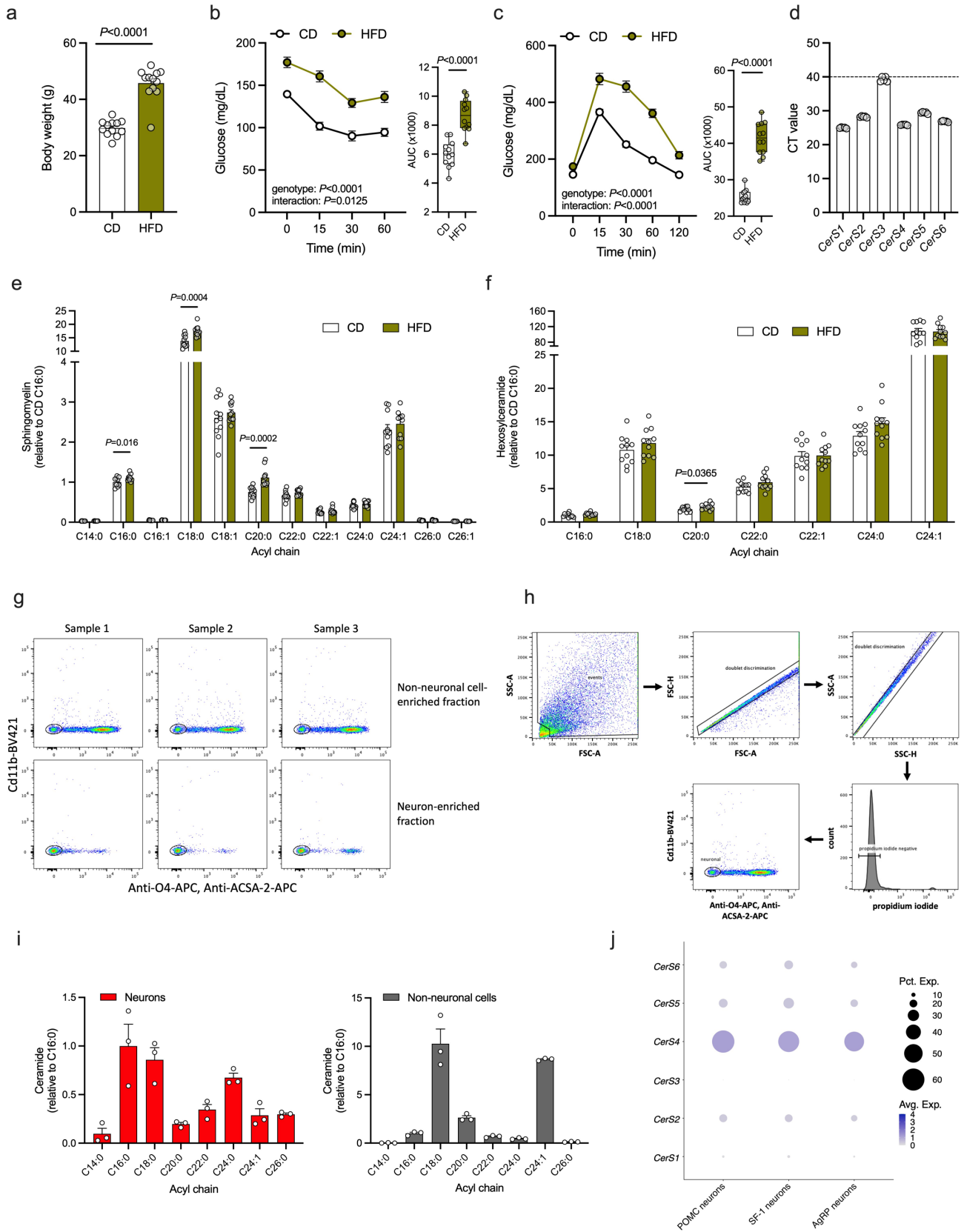


## Supplementary Information

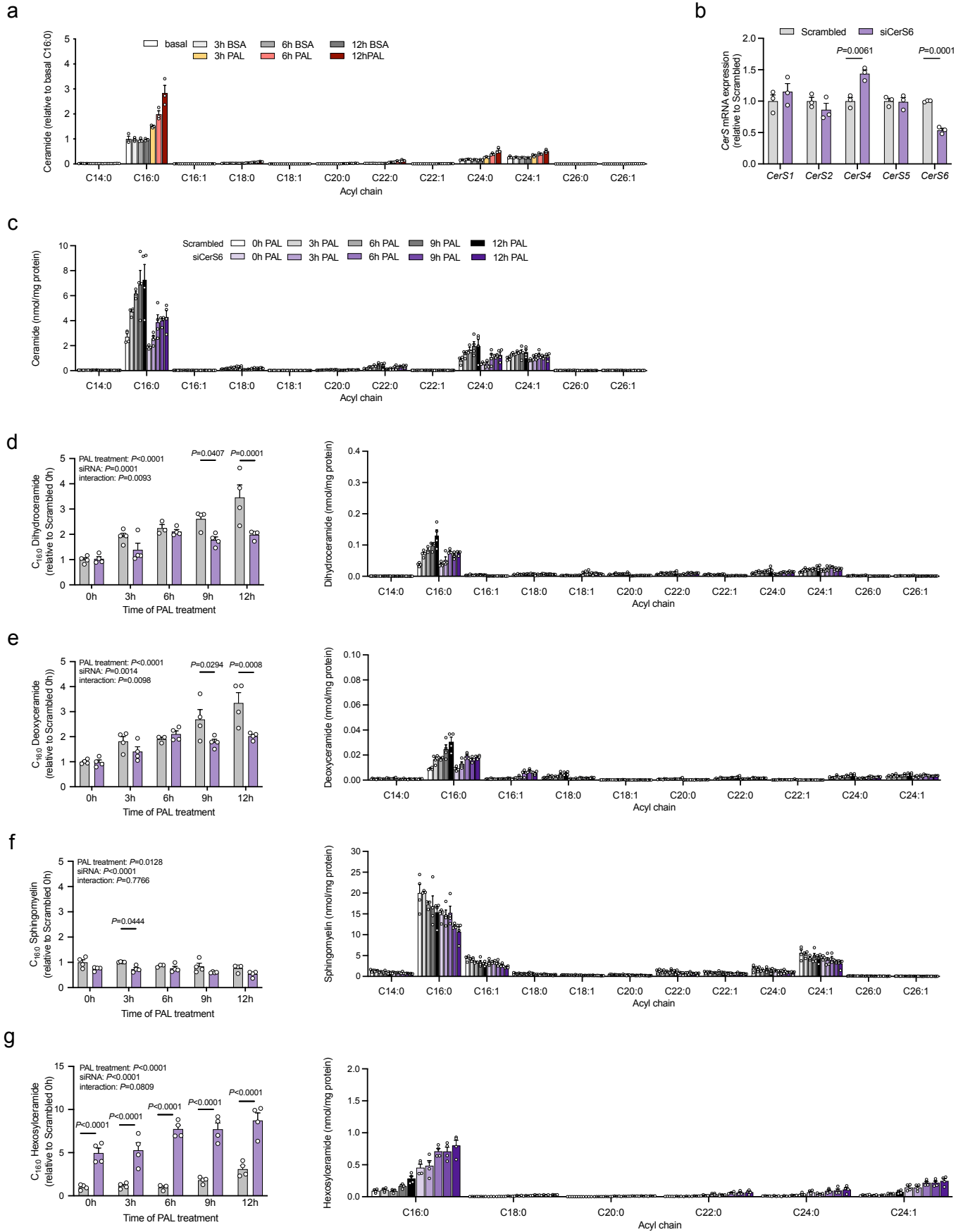
CerS6-dependent ceramide synthesis in hypothalamic neurons promotes ER/mitochondrial stress and impairs glucose homeostasis in obese mice

Philipp Hammerschmidt, Sophie M. Steculorum, Cécile L. Bandet, Almudena Del Río-Martín, Lukas Steuernagel, Vivien Kohlhaas, Marvin Feldmann, Luis Varela, Adam Majcher, Marta Quatorze Correia, Rhena F. U. Klar, Corinna A. Bauder, Ecem Kaya, Marta Porniece-Kumar, Nasim Biglari, Anna Sieben, Tamas L. Horvath, Thorsten Hornemann, Susanne Brodesser, Jens C. Brüning



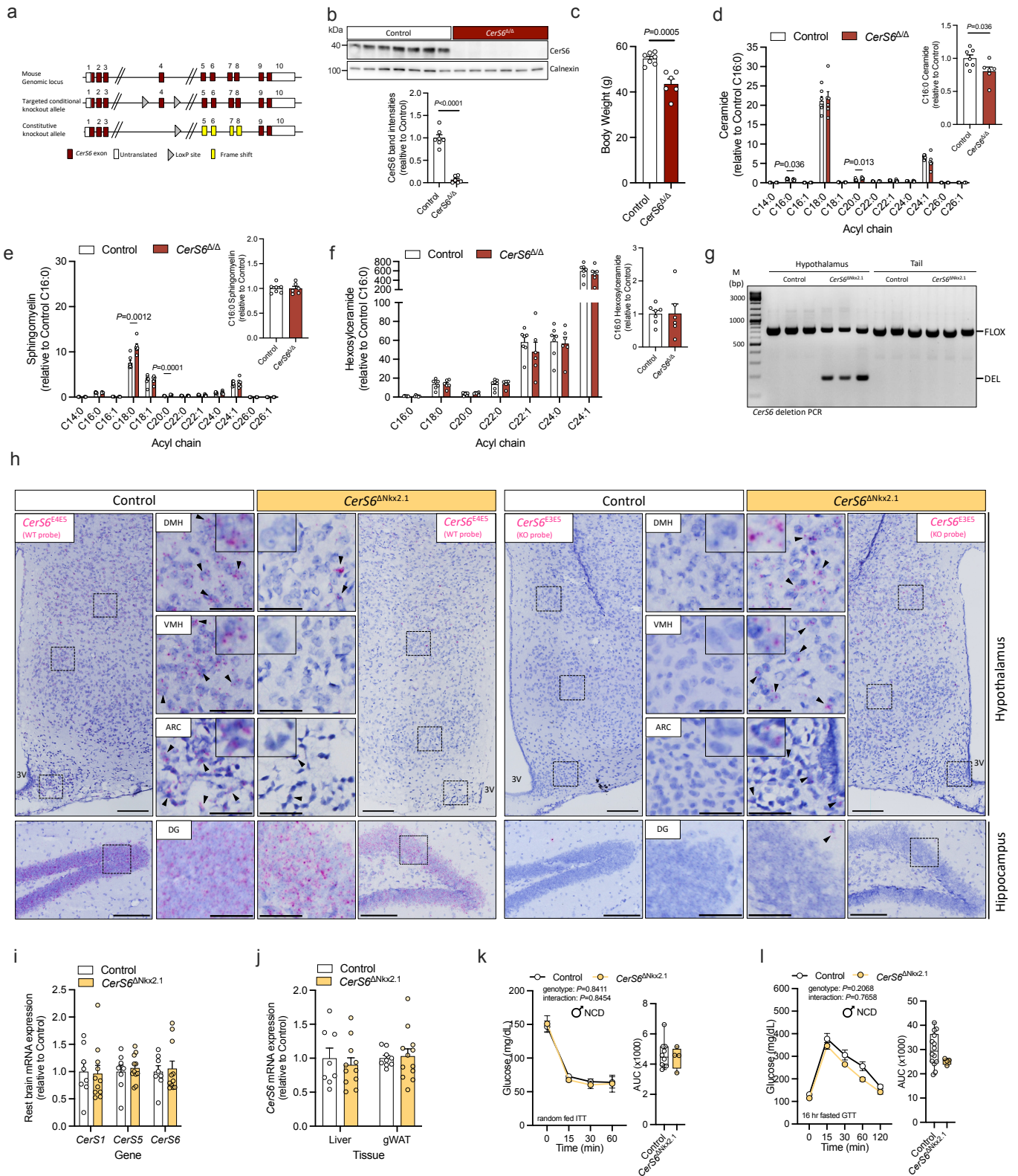
**Supplementary Fig. 1: Metabolic characterization, sphingolipid levels, and CerS expression in C57BL/6N mice fed a control or high-fat diet. (Related to Fig. 1)**

**a-c**, Metabolic characterization of C57BL/6N male mice used for analysis of CerS6 protein expression and sphingolipid content in hypothalamus homogenates. Mice fed *ad libitum* with a control diet (CD) or high-fat diet (HFD) for 16 weeks. **a**, Body weight of mice at 20 weeks of age when sacrificed for organ collection (n=12 mice/group). **b**, Insulin tolerance test at 16 weeks of age and area under the curve (AUC) for each mouse (n=12 mice/group). **c**, Glucose tolerance test following a 6 hr fasting period at 17 weeks of age and AUCs (n=12 mice/group). **d**, Cycle threshold (CT) values of qPCR analysis in hypothalamus homogenates of misty control mice using TaqMan probes targeting the different CerS mRNAs. Dashed line indicates detection threshold at 40 cycles (n=5 mice). **e, f**, Lipidomic analysis of sphingomyelin (**e**) and hexosylceramide species (**f**) in hypothalamus homogenates of CD- and HFD-fed mice relative to the respective C<sub>16:0</sub> sphingolipid species in CD-fed mice (n=11 mice/group). **g**, Flow cytometry-based analysis for non-neuronal cell markers CD11b (microglia, y axis), O4 (oligodendrocytes, x axis), and ACSA-2 (astrocytes, x axis) in non-neuronal cell- (upper row) and neuron-enriched cell fractions (lower row) isolated from the hypothalamus of three normal chow-fed mice (Samples 1-3), respectively. FACS plot only demonstrates cell type purity but has no and requires no statistical analysis. **h**, Representative dot plots illustrate the gating strategy used to verify the neuronal and non-neuronal fractions shown in **g**. After doublet discrimination (FSC-H vs. FSC-A, SSC-A vs. SSC-H), dead cells were excluded based on propidium iodide fluorescence. Non-neuronal cells were excluded using CD11b, O4, and ACSA-2 markers. **i**, Lipidomic analysis of ceramides in the neuron-enriched cell fraction (red, Neurons) and non-neuronal cell-enriched fraction (grey, Non-neuronal cells) (n=3 mice). **j**, Dot plots of CerS1-6 expression in POMC-, SF-1-, and AgRP-expressing neurons according to single-cell sequencing results harmonized in HypoMap. Data in **a, d-f, i**, and longitudinal data in **b, c** are represented as mean values  $\pm$ SEM. Boxplots indicate median  $\pm$ min/max and include data points of individual mice entering the analysis. *P* values calculated using two-tailed unpaired Student's *t*-test (**a, e, f**, AUCs in **b, c**) or two-way RM ANOVA (longitudinal analysis in **b, c**). Source data and further details of statistical analyses are provided as a Source Data file.



**Supplementary Fig. 2: CerS6 in mHypoE-N43/5 cells. (Related to Fig. 2)**

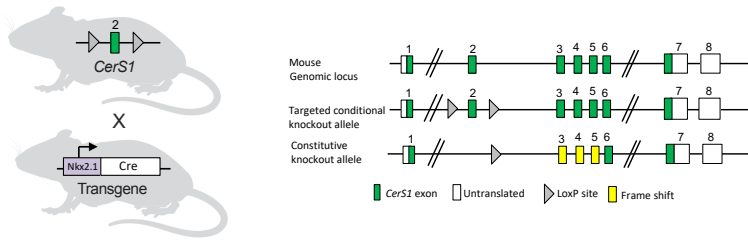
**a**, Relative ceramide levels in N43/5 cells that were either left untreated (basal) or exposed to palmitate (PAL, 500  $\mu$ M) or BSA for the time indicated (n=3 independent cultures). Values are expressed relative to the C<sub>16:0</sub> ceramide content at basal conditions. **b**, Relative mRNA expression of *CerS1-6* in N43/5 cells treated with siCerS6 (purple) or scrambled (grey, n=3 independent cultures with 3 replicate dishes/experiment). **c**, Absolute ceramide levels in siCerS6- or scrambled treated N43/5 cells incubated with PAL for the time indicated in hours (h) (n=4 independent cultures). **d-g**, C<sub>16:0</sub> sphingolipid species relative to levels at 0h BSA (left) and absolute levels (right) of dihydroceramides (**d**), deoxyceramides (**e**), sphingomyelins (**f**), and hexosylceramides (**g**) (n=4 independent cultures). Data are represented as mean values  $\pm$ SEM. *P* values calculated using two-tailed unpaired Student's *t*-test (**b**) or two-way ANOVA and Bonferroni's multiple comparison test (C<sub>16:0</sub> sphingolipid levels in **d-g**). Source data and further details of statistical analyses are provided as a Source Data file.



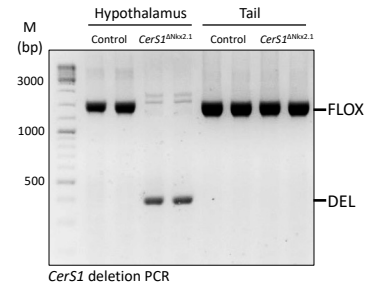
**Supplementary Fig. 3: CerS6 deficiency in the hypothalamus and in hypothalamic neurons of mice. Related to Fig. 3**

**a**, Simplified schematic illustration detailing deletion of exon 4 of the *CerS6* gene via Cre-loxP-mediated DNA recombination. **b**, Immunoblot analysis of CerS6 in hypothalamus homogenates of HFD-fed control (white) and HFD-fed conventional CerS6 knockout male mice (*CerS6*<sup>ΔΔ</sup>, red); CerS6 band intensities normalized for Calnexin and expressed as relative to control (n=7vs.6 mice). Uncropped blots in Source Data. **c**, Body weight of mice when sacrificed for organ collection (n=7vs.6 mice). **d-f**, Levels of ceramides (**d**), sphingomyelins (**e**), and hexosylceramides (**f**) in the hypothalamus of HFD-fed control and *CerS6*<sup>ΔΔ</sup> mice relative to the respective C<sub>16:0</sub> sphingolipid species in controls (n=7vs.6 mice). Relative levels of C<sub>16:0</sub> ceramide, sphingomyelin, or hexosylceramide are highlighted separately. **g**, PCR analysis on genomic DNA for exon 4 deletion of *CerS6* in extracts of the hypothalamus and tail of *CerS6*<sup>ΔNkx2.1</sup> mice and controls (n=3 mice/group). **h**, Brightfield images of BaseScope in situ hybridization using a probe targeting the exon junction 4/5 in the *CerS6* transcript (*CerS6*<sup>E4E5</sup>, red), illustrating expression of full-length *CerS6* (left), or the exon junction 3/5 (*CerS6*<sup>E3E5</sup>, red), illustrating expression of the recombined exon 4-deficient transcript of *CerS6* (right) in the hypothalamus (top) and hippocampus (bottom) of *CerS6*<sup>ΔNkx2.1</sup> mice (orange) and controls (white); zoom images depict the dorsomedial nucleus (DMH), ventromedial nucleus (VMH), arcuate nucleus (ARC) of the hypothalamus, and the dentate gyrus (DG) of the hippocampus; blue denotes nuclei stained by haematoxylin; dashed squares indicate zoom range; black arrows depict cells positive for the respective *CerS6* transcript; 3V, third ventricle; scale bars: 150 μm for overview images, 50 μm for zoom images. **i**, Relative mRNA expression of *CerS1*, *CerS5*, and *CerS6* in brain homogenates excluding the hypothalamus analyzed by qPCR in HFD-fed control and *CerS6*<sup>ΔNkx2.1</sup> mice (n=8vs.11 mice). **j**, Relative mRNA expression of *CerS6* in liver (n=8vs.11 mice) and gonadal white adipose tissue (gWAT) of control and *CerS6*<sup>ΔNkx2.1</sup> mice (n=9vs.12 mice). **k, l**, Insulin tolerance test (ITT) in random-fed mice (**k**, n=10vs.4 mice) and glucose tolerance test (GTT) after a 16 hr fasting period (**l**, n=14vs.4 mice) in NCD-fed controls and *CerS6*<sup>ΔNkx2.1</sup> mice. All data obtained from male mice. Data in b-j and longitudinal data in k, l are represented as mean values ±SEM. Boxplots indicate median ±min/max and include data points of individual mice entering the analysis. *P* values calculated using two-tailed unpaired Student's *t*-test (**b-e**) and two-way RM ANOVA (longitudinal analysis in **k, l**). Source data and further details of statistical analyses are provided as a Source Data file.

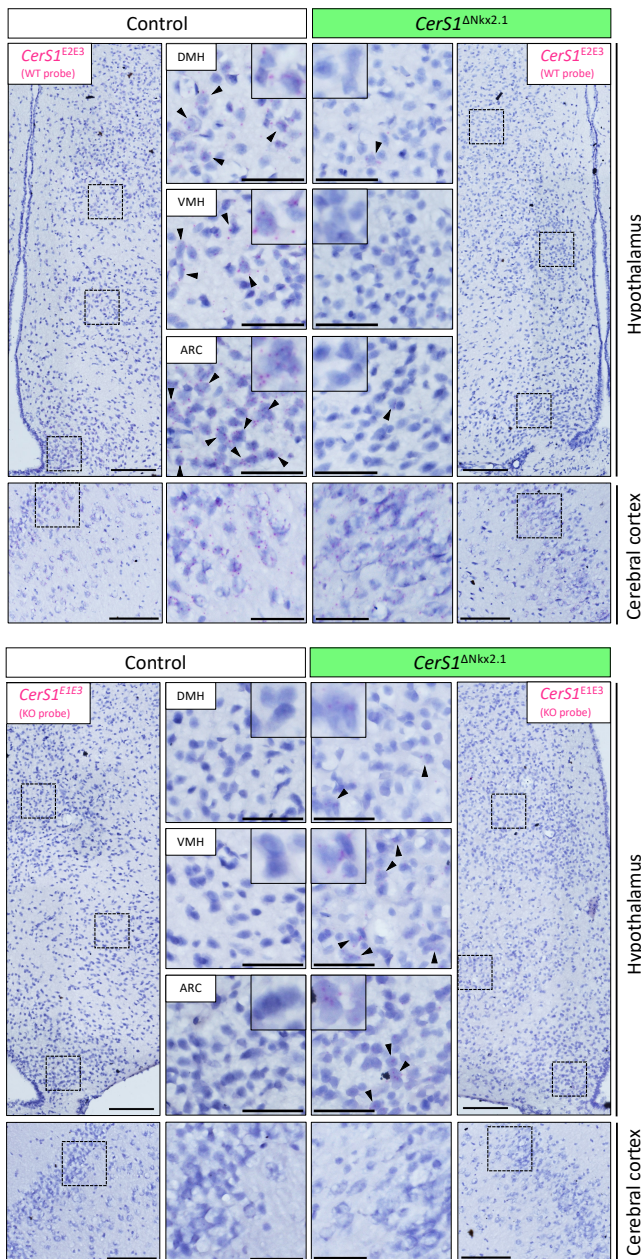
a



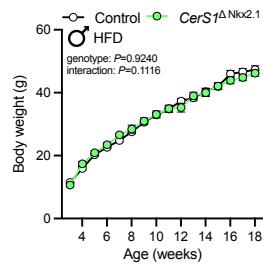
b



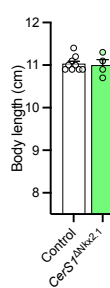
c



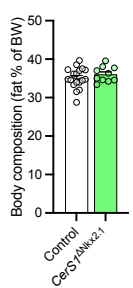
d



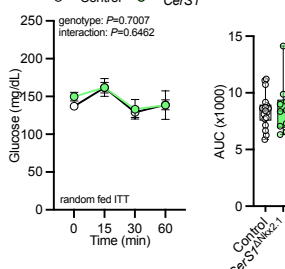
e



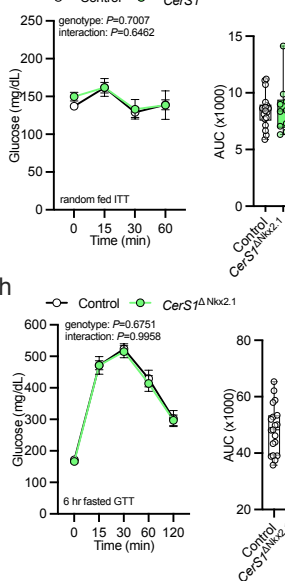
f



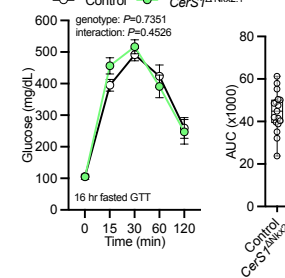
g



h



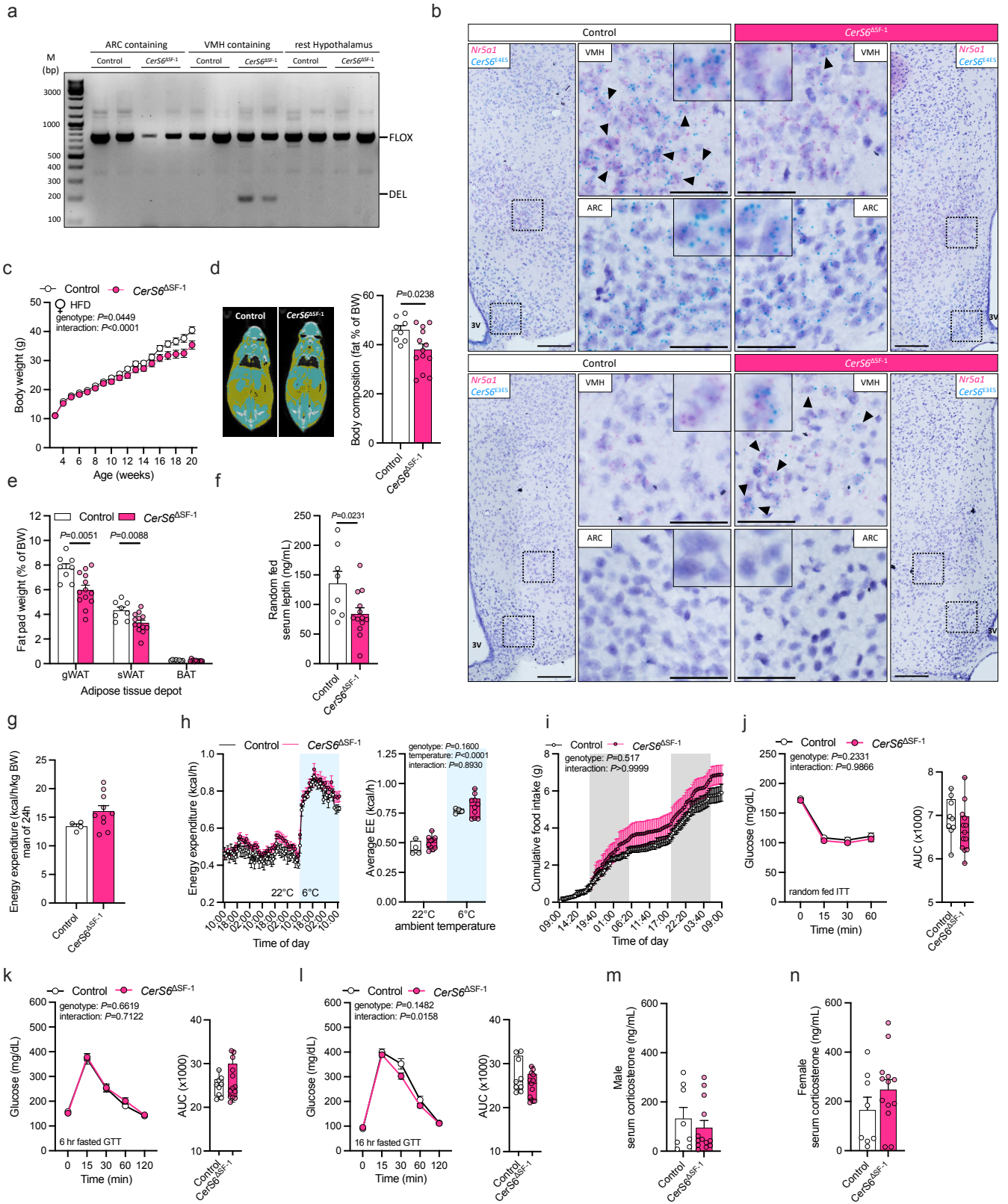
i





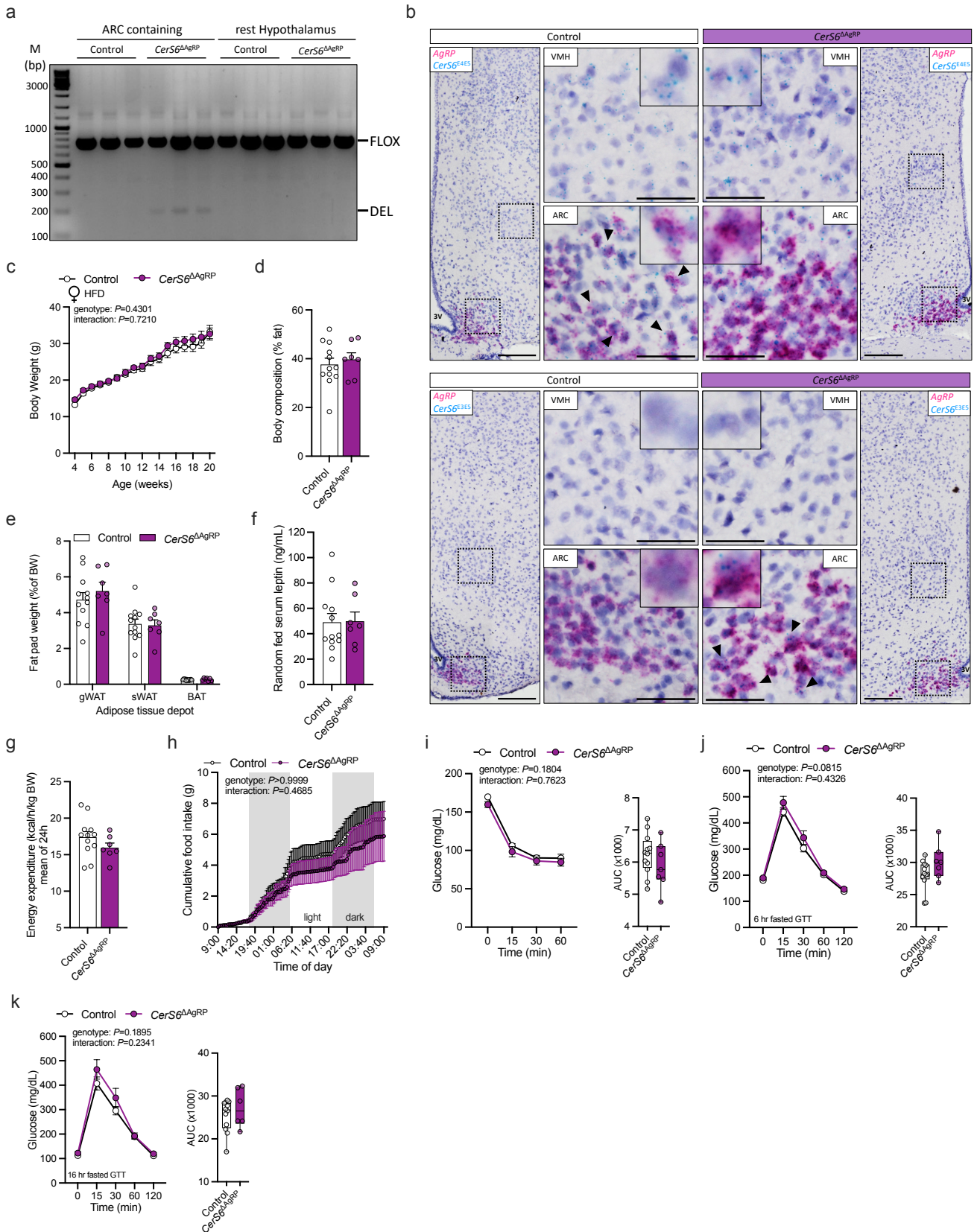
**Supplementary Fig. 4: Depletion of CerS1 in hypothalamic neurons does not affect glucose metabolism in obesity. Related to Fig. 3**

**a**, Left: *CerS1<sup>fl/fl</sup>* mice in which exon 2 of *CerS1* (green) is flanked by loxP sites (grey triangles) were bred to mice with transgenic Cre expression (white) under control of the Nkx2.1 promoter (purple). Right: Excision of exon 2 in *CerS1* leads to a frameshift in the downstream exons 3-5, preventing translation of the functional domain responsible for ceramide synthesis. *CerS1<sup>fl/fl</sup>* mice expressing Nkx2.1-Cre (*CerS1<sup>ΔNkx2.1</sup>*, bright green) and Cre-negative *CerS1<sup>fl/fl</sup>* littermates (Control, white) were used for analysis. **b**, PCR analysis on genomic DNA for exon 2 deletion of *CerS1* in extracts of the hypothalamus and tail of *CerS1<sup>ΔNkx2.1</sup>* mice and controls (n=2 mice/group). **c**, Brightfield images of in situ hybridization using a BaseScope probe targeting the exon junction 2/3 in the *CerS1* transcript (*CerS1<sup>E2E3</sup>*, red), illustrating expression of full-length *CerS1* (top), or a probe targeting the exon junction 1/3 (*CerS1<sup>E1E3</sup>*, red), illustrating expression of the recombined exon 2-deficient transcript of *CerS1* (bottom) in the hypothalamus (top) and cerebral cortex (bottom) of *CerS1<sup>ΔNkx2.1</sup>* mice and controls; zoom images depict the dorsomedial nucleus (DMH), ventromedial nucleus (VMH), and arcuate nucleus (ARC) of the hypothalamus; blue denotes nuclei stained by haematoxylin; dashed squares indicate zoom range; black arrows depict cells positive for the respective *CerS1* transcript; 3V, third ventricle; scale bars: 150 μm for overview images, 50 μm for zoom images. **d**, Body weight development of male mice during HFD feeding (n=8-19 mice/group and week), **e**, Body length (n=9vs.4 mice), and **f**, body fat content relative to body weight, measured by nuclear magnetic resonance (n=18vs.10 mice). **g**, Insulin tolerance test and area under the curve (AUC) for each mouse (n=18vs.10 mice), **h**, glucose tolerance test following a 6 hr fasting period and AUCs (n=19vs.13 mice), and **i**, glucose tolerance test following a 16 hr fasting period and AUCs (n=17vs.8 mice). All data obtained from male mice. Data in **d-f** and longitudinal data in **g-i** are represented as mean values ±SEM. Boxplots indicate median ±min/max and include data points of individual mice entering the analysis. *P* values calculated using a mixed-effects model (**d**) or two-way RM ANOVA (longitudinal analysis in **g-i**). Source data and further details of statistical analyses are provided as a Source Data file. Created with BioRender.com.



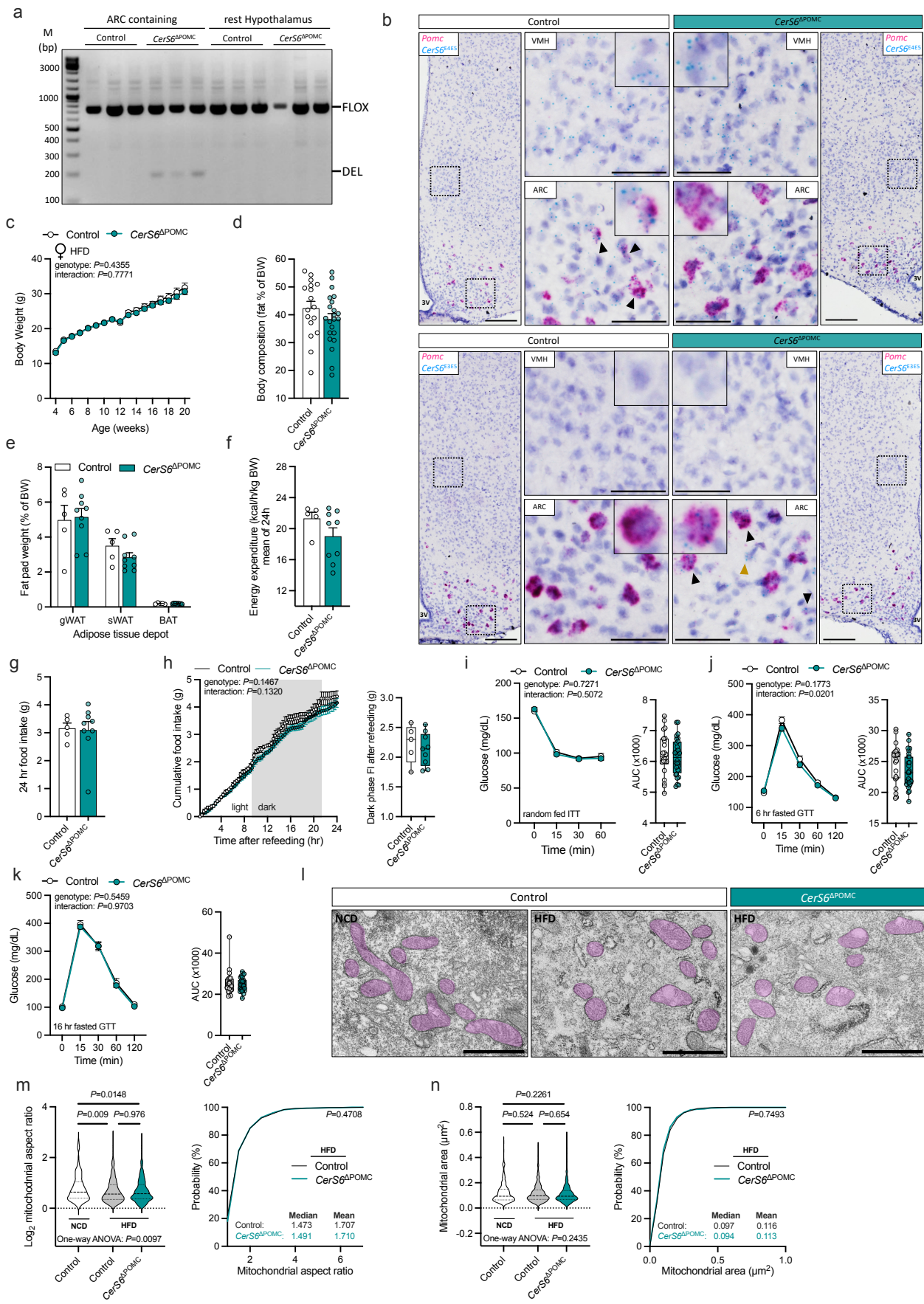
**Supplementary Fig. 5: Depletion of CerS6 in SF-1 neurons reduces adiposity in HFD-fed female mice. Related to Fig. 4**

**a**, PCR analysis on genomic DNA for exon 4 deletion of *CerS6* in ARC- and VMH-containing tissue samples and the rest of the hypothalamus of control and *CerS6*<sup>ΔSF-1</sup> mice (n=2 mice/group). **b**, Brightfield images of BaseScope duplex in situ hybridization using probes targeting *Nr5a1* (encoding SF-1, red) and the exon junction 4/5 in the *CerS6* transcript (*CerS6*<sup>E4E5</sup>), illustrating expression of full-length *CerS6* (bright blue, top), or the exon junction 3/5 (*CerS6*<sup>E3E5</sup>), illustrating expression of the recombined exon 4-deficient transcript of *CerS6* (bright blue, bottom) in the hypothalamus of *CerS6*<sup>ΔSF-1</sup> mice (pink) and controls (white); zoom images depict the ventromedial nucleus (VMH) and arcuate nucleus (ARC) of the hypothalamus; blue denotes nuclei stained by haematoxylin; dashed squares indicate zoom range; black arrows depict cells coexpressing *Nr5a1* and the respective *CerS6* transcript; 3V: third ventricle; scale bars: 150 μm for overview images, 50 μm for zoom images. **c-l**, Analysis of HFD-fed control (white) and *CerS6*<sup>ΔSF-1</sup> female mice (pink). **c**, Body weight development of mice during HFD feeding (n=9vs.13 mice/weeks 3-13, n=8vs.13 mice/weeks 14-20). **d**, CT scans (yellow, fat tissue; blue, non-adipose soft tissue) and quantification of body fat content relative to body weight (n=8vs.13 mice). **e**, Fat-pad weights of gonadal white adipose tissue (gWAT, n=8vs.13 mice), subcutaneous WAT (sWAT, n=8vs.13), and brown adipose tissue (BAT, n=8vs.12) relative to body weight. **f**, Serum leptin levels of random-fed mice (n=8vs.13 mice). **g**, Average energy expenditure over 24 hr normalized for body weight (n=4vs.10 mice). **h**, Absolute energy expenditure (EE) at 22°C ambient temperature and upon exposure to 6°C, over time (left) and in average (right, n=4vs.10 mice). **i**, Cumulative food intake over 48 hr (n=4vs.10 mice; grey background indicates dark phase). **j**, Insulin tolerance test and area under the curve (AUC) for each mouse (n=9vs.13 mice). **k, l**, Glucose tolerance test following a 6 hr (**k**) or 16 hr (**l**) fasting period and AUCs (n=9vs.13 mice). **m, n**, Serum corticosterone levels in random-fed male (**m**) and female (**n**) mice (n=8vs.13 mice/sex). All data in **c-l** obtained from female mice. Data in **c-g, m, n**, and longitudinal data in **h-l** are represented as mean values ±SEM. Boxplots indicate median ±min/max and include data points of individual mice entering the analysis. *P* values calculated using two-tailed unpaired Student's *t*-test (**d-f**), two-way ANOVA and Bonferroni's multiple comparison test (Average EE in **h**), two-way RM ANOVA (longitudinal analysis in **j-l**), or a mixed-effects model (**c**). Source data and further details of statistical analyses are provided as a Source Data file.



**Supplementary Fig. 6: Depletion of CerS6 in AgRP neurons does not affect glucose and energy metabolism in HFD-fed female mice. Related to Fig. 5**

**a**, PCR analysis on genomic DNA for exon 4 deletion of *CerS6* in ARC-containing tissue samples and the rest of the hypothalamus of control and *CerS6*<sup>ΔAgRP</sup> mice (n=3 mice/group). **b**, Brightfield images of BaseScope duplex in situ hybridization using probes targeting *Agrp* (red) and the exon junction 4/5 in the *CerS6* transcript (*CerS6*<sup>E4E5</sup>), illustrating expression of full-length *CerS6* (bright blue, top), or the exon junction 3/5 (*CerS6*<sup>E3E5</sup>), illustrating expression of the recombinant exon 4-deficient transcript of *CerS6* (bright blue, bottom) in the hypothalamus of *CerS6*<sup>ΔAgRP</sup> mice (purple) and controls (white); zoom images depict the ventromedial nucleus (VMH) and arcuate nucleus (ARC) of the hypothalamus; blue denotes nuclei stained by haematoxylin; dashed squares indicate zoom range; black arrows depict cells coexpressing *Agrp* and the respective *CerS6* transcript; 3V: third ventricle; scale bars: 150 μm for overview images, 50 μm for zoom images. **c-k**, Analysis of HFD-fed control (white) and *CerS6*<sup>ΔAgRP</sup> (purple) female mice. **c**, Body weight development of mice during HFD feeding (n=3-12 mice/group and week). **d**, Body fat content relative to body weight measured by micro-CT analysis (n=12vs.7 mice). **e**, Fat-pad weights of gonadal white adipose tissue (gWAT), subcutaneous WAT (sWAT), and brown adipose tissue (BAT) relative to body weight (n=12vs.7 mice). **f**, Serum leptin levels of random-fed mice (n=12vs.7 mice). **g**, Average energy expenditure over 24 hr normalized for body weight (n=12vs.7 mice). **h**, Cumulative food intake over 48 hr (n=12vs.7 mice; grey background indicates dark phase). **i**, Insulin tolerance test and area under the curve (AUC) for each mouse (n=12vs.7 mice), **j**, glucose tolerance test following a 6 hr fasting period and AUCs (n=12vs.7 mice), and **k**, glucose tolerance test following a 16 hr fasting period and AUCs (n=12vs.6 mice). All data in (**c-k**) obtained from female mice. Data in **c-g**, and longitudinal data in **i-k** are represented as mean values ±SEM. Boxplots indicate median ±min/max and include data points of individual mice entering the analysis. *P* values calculated using two-way RM ANOVA (longitudinal analysis in **h**, **i-k**) or a mixed-effects model (**c**). Source data and further details of statistical analyses are provided as a Source Data file.



**Supplementary Fig. 7: Depletion of CerS6 in POMC neurons does not affect mitochondrial morphology, feeding behavior, and glucose metabolism in HFD-fed female mice.**

**Related to Fig. 6**

**a**, PCR analysis on genomic DNA for exon 4 deletion of *CerS6* in ARC-containing tissue samples and the rest of the hypothalamus of control and *CerS6*<sup>ΔPOMC</sup> mice (n=3 mice/group). **b**, BaseScope duplex in situ hybridization using probes targeting *Pomc* (red) and the exon junction 4/5 in the *CerS6* transcript (*CerS6*<sup>E4E5</sup>), illustrating expression of full-length *CerS6* (bright blue, top), or the exon junction 3/5 (*CerS6*<sup>E3E5</sup>), illustrating expression of the recombined exon 4-deficient transcript of *CerS6* (bright blue, bottom) in the hypothalamus of *CerS6*<sup>ΔPOMC</sup> mice (green) and controls (white); zoom images depict the ventromedial nucleus (VMH) and arcuate nucleus (ARC) of the hypothalamus; blue denotes nuclei stained by haematoxylin; dashed squares indicate zoom range; black arrows depict cells coexpressing *Pomc* and the respective *CerS6* transcript and yellow arrow depicts a *Pomc*-negative cell with expression of the exon 4-deficient transcript in the ARC of *CerS6*<sup>ΔPOMC</sup> mice; 3V: third ventricle; scale bars: 150 μm for overview images, 50 μm for zoom images. **c-n**, Analysis of HFD-fed control (white) and *CerS6*<sup>ΔPOMC</sup> (green) female mice. **c**, Body weight development of mice during HFD feeding (n=10-28 mice/group and week). **d**, Body fat content relative to body weight measured by micro-CT analysis (n=17vs.22 mice). **e**, Fat-pad weights of gonadal white adipose tissue (gWAT), subcutaneous WAT (sWAT), and brown adipose tissue (BAT) relative to body weight (n=5vs.9 mice). **f**, Average energy expenditure over 24 hr normalized for body weight (n=5vs.9 mice). **g**, Absolute food intake over 24 hr (n=5vs.9 mice). **h**, Cumulative food intake after refeeding following a 16 hr fasting period (grey background indicates dark phase) and quantification of absolute food intake (FI) during the dark phase after refeeding (n=5vs.9 mice). **i**, Insulin tolerance test and area under the curve (AUC) for each mouse (n=22vs.28 mice). **j, k**, Glucose tolerance test following a 6 hr (**j**) or 16 hr (**k**) fasting period and AUCs (n=22vs.28 mice). **l**, Representative transmission electron micrographs of mitochondria in ARC POMC neurons of control female mice fed a normal chow (NCD, left) or high-fat diet (HFD, middle), and HFD-fed *CerS6*<sup>ΔPOMC</sup> mice (right); scale bars: 1 μm. **m**, Violin plots of log<sub>2</sub>-transformed mitochondrial aspect ratios (n=221-843 mitochondria/group from 5-6 POMC neurons/mouse, 1-3 mice/group) and cumulative distribution function (probability plot) of mitochondrial aspect ratios in HFD-fed *CerS6*<sup>ΔPOMC</sup> mice and controls (n=774-843 mitochondria/group from 5-6 POMC neurons/mouse, 3 mice/group). **n**, Violin plots of mitochondrial area (n=221-843 mitochondria/group from 5-6 POMC neurons/mouse, 1-3 mice/group) and cumulative distribution function (probability plot) of mitochondrial area in HFD-fed *CerS6*<sup>ΔPOMC</sup> mice and control littermates (n=774-843 mitochondria/group from 5-6 POMC neurons/mouse, 3 mice/group). All data in **c-n** obtained from female mice. Data in **c-g** and longitudinal data in **h-k** are represented as mean values ±SEM. Boxplots indicate median ±min/max and include data points of individual mice entering the analysis. Dashed lines in violin plots indicate median and dotted lines indicate the first and third quartile, respectively. *P* values calculated using one-way ANOVA followed by Tukey's multiple comparison test (**m, n**), Kolmogorov-Smirnov test (distributions in **m, n**), two-way RM ANOVA (longitudinal analysis in **h, i-k**), or a mixed-effects model (**c**). Source data and further details of statistical analyses are provided as a Source Data file.